Self-assembling of dry and cohesive non-Brownian spheres

O. Carvente[1] and J. C. Ruiz-Suárez[2,*]

[1]*Departamento de Física Aplicada, CINVESTAV-Mérida, Apartado Postal 73 Cordemex, Mérida, Yucatán 97310, Mexico*

[2]*CINVESTAV-Monterrey, Autopista Nueva al Aeropuerto Km 9.5, Apodaca, Nuevo León 66600, Mexico*

(Received 10 August 2007; published 11 July 2008)

Numerous experimental and computational studies have been carried out in recent years to understand the mechanisms governing the compaction of granular systems. Here the problem is further investigated from a different perspective. We compact spheres by a vibrational annealing method and show how the interactions between them and the walls determine the final structure. Dry spheres self-assemble only in body-centered-tetragonal structures, while cohesive ones surpass such density and reach the most compact face-centered-cubic phase. We argue that such polymorphism is due to a molecularlike behavior induced by a compensation mechanism between free and vibrational energies.

DOI: 10.1103/PhysRevE.78.011302 PACS number(s): 45.70.Cc, 45.50.−j

I. INTRODUCTION

Granular systems are normally found in disordered states and in repose. The two conditions are related: grains are non-Brownian particles and therefore, under the influence of gravity, they find mechanical equilibrium at random configurations. However, such random structures relax into many others when they are slightly perturbed, following a dynamic behavior characterized by hierarchical relaxation phenomena with different time scales [1–3]. Over the last five decades, the scientific efforts aimed at understanding the mechanisms behind granular relaxation have been enormous. We know today, for instance, that vibrated spherical grains compact in random-close-packed (rcp) configurations [4], that they reach such phases in a logarithmic fashion [5], that their compactivity drops when the volume fraction increases [6], and that aggregates of face-adjacent tetrahedra are the essential feature of dense disordered packings [7]. We know as well that granular assembling may occur under special vibration or shearing conditions [8–11]. But, despite the accumulated knowledge, granular relaxation is still a conundrum.

In order to clarify our understanding on this subject, we must look into related phenomena occurring at other scales. In microscopic systems, for example, molecular packing has a very well-established grammar [12], which is based on a simple but powerful relationship: $G=E-TS$. This expression determines how entropy (S) and enthalpy (E), at a given temperature T, compete to determine the free energy (G) of the system. An equivalent relationship is $A=U-TS$, where A is the Helmholtz free energy and U the internal energy of the system. We use one or the other depending on whether the pressure or temperature is constant.

The balance between entropy and enthalpy (or internal energy) plays a fundamental role in the thermodynamic behavior of physical, chemical, and biological systems [13–15]. The mechanism is simple [15]: when the well of the interaction potential between the constituents of the system is deep (i.e., when the intermolecular attraction is strong), vibrational entropy is hindered and the free energy increases. However, when the attraction is weak, entropy prevails.

This conceptual framework has also been used in mesoscopic systems. After years of debate, it has been finally understood why a colloidal hard-sphere suspension, where particles do not interact and therefore enthalpy (or internal energy) is zero, crystallizes. The rationale is the following [16–18]: when a suspension is prepared at high concentrations, particles are geometrically arrested and barely move (vibrational entropy is zero); however, there is a tendency for the system to optimize G and the only way to do this is by increasing the entropy. Enthalpy is nonexistent because hard spheres do not interact, yet crystallization occurs due to the increase of entropy (when the system crystallizes, particles are now free to erratically oscillate around their equilibrium positions).

Can we extend these ideas to understand the self-assembly of granular systems? This is the question we would like to answer here. We have recently carried out experiments on granular crystallization and reported our findings in two previous contributions [9,10]. In the following we give a brief account of such results.

We have shown that hexagonal-close-packed (hcp) structures can be obtained by an epitaxial technique in triangular confinement [9]. In this technique, particles are incorporated while the system vibrates, and self-assembly occurs layer by layer in a sequence of planes $ABABA\ldots$, according to the standard description of close-packed polytypes. Face-centered-cubic (fcc) structures are not commensurable in such confinements and for this reason their growth is geometrically forbidden (the same happens with hcp structures in square boxes). Thus, in order to self-assemble fcc structures by this epitaxial technique, we must look for the right confinement. What happens, however, in closed systems (i.e., when all the particles are already inside the container)? Is it possible to transit from a disordered to an ordered phase? To answer this question some previous works have been carried out [8,10,11]. We have reported, for instance, that self-assembly in closed systems is possible if vibrational annealing (VA) is used [10]. The method consists in shaking the granular assembly with a sinusoidal vibration; where the frequency ν (amplitude A) is continuously increased (decreased) in such a way that the dimensionless acceleration $\Gamma=A(2\pi\nu)^2/g$ remains constant. At the beginning of the vi-

*cruiz@mda.cinvestav.mx

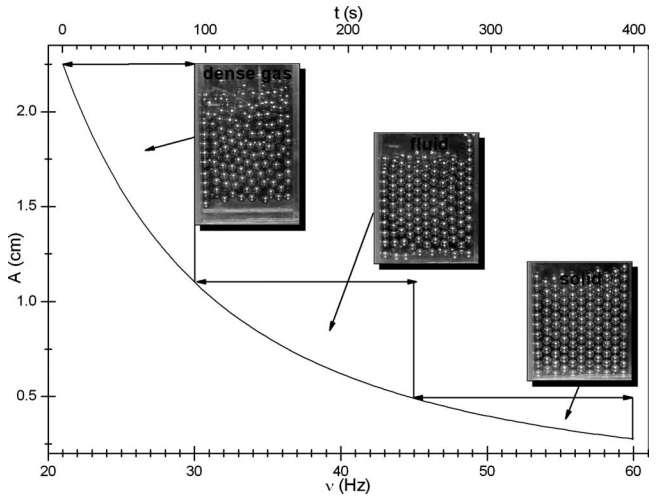

FIG. 1. The vibrational annealing method. It consists in a programmed sinusoidal vibration given by a hyperbolic function at constant Γ. At large amplitudes (and low frequencies) the system is a steady-state dense gas. Thereafter, at intermediate values of amplitudes and frequencies, the system becomes a fluid where convection is clearly observed. Finally, at small amplitudes (high frequencies) the system is a vibrating solid, where fractures are annealed away to form a single crystal. The time scale is only illustrative; it gives an idea of the usual cooling rate to achieve crystallization. As long as the three phases described above are observed, other cooling rates give similar results.

bration, when the amplitude is large and the frequency small, most of the assembly is a dense gas. Slowly, the assembly becomes a fluidlike system where the beads reduce their velocity but still move all around the container. Finally, at high frequencies and small amplitudes, the system is a solid where beads only vibrate around their equilibrium positions. At this stage fractures are annealed away and a perfect crystal forms. In Fig. 1 we depict the mentioned evolution (the solid line is the hyperbola A vs ν with $\Gamma=3$). Using this technique, we have discovered that dry beads in rectangular confinements self-assemble in body-centered-tetragonal (bct) structures, while cohesive beads form fcc crystals [10].

In this contribution, we advance our understanding in this matter, claiming that a mechanism analogous to the entropy-enthalpy compensation principle (used in microscopic systems [15]) might be at the source of the observed granular polymorphism. Experiments are carried out, and the results thoroughly discussed, to sustain this idea.

II. EXPERIMENTAL DETAILS

The experimental setup is a vertical shaking system driven by a function generator (HP-33120A), an amplifier, and a controlling computer. The initial conditions of the annealing (amplitude and frequency), and the rate of the cooling program, are given to the computer at the beginning of the process. As long as the annealing rate is not too fast to quench the system in a disordered structure, this rate is not crucial. Rectangular plexiglass cells (the dimensions of which go from 2.54 to 12 cm per side and 20 cm in height)

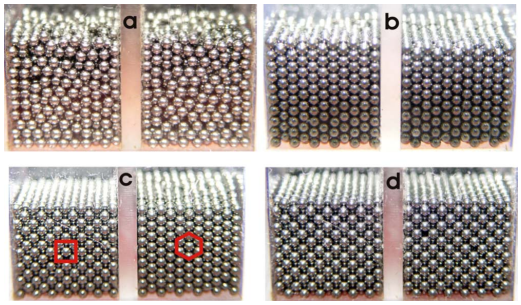

FIG. 2. (Color online) Monodisperse beads in a double container. There are 1100 ball bearings (1.56 mm diameter) in each vessel. (a) Randomly packed in each vessel; (b) after the vibrational annealing, bct in both vessels; (c) 20 μl of oil, with viscosity 1 cP, were added to the left vessel before the annealing process. The cohesion produced by the oil triggers the formation of a fcc structure. In the right vessel the spheres are dry and the bct structure forms again. (d) 20 μl of oil, with viscosity 1 cP, were added to the right vessel before the annealing process. Now the spheres are wet in both vessels and fcc lattices are formed.

are used in the experiments. Other experimental details of this work are given throughout the paper.

III. GRANULAR POLYMORPHISM

Our first experiment aims to reproduce the results reported in [10] in a different fashion. It deals with the simultaneous assembling of spherical beads in a container with two identical vessels. Figure 2(a) shows these vessels charged with monodisperse ball bearings (equal quantities in each one). After an annealing similar to the one depicted in Fig. 1, bct structures are formed in each one of the compartments [Fig. 2(b)]. Both of them have a width of five primitive cells, and the planes parallel to the walls are hexagonal. This type of structure leaves channels along the vertical axis (it is translucent along this direction) and therefore it is not optimally compacted. The packing fraction of an infinite bct structure is 0.69, which is smaller than 0.74, the highest packing fraction corresponding to the fcc structure.

Repeating exactly the same annealing process, but previously adding to the left vessel several drops of oil [19], we obtain two different phases: fcc and bct [see Fig. 2(c)]. The assemblies are simultaneously annealed in the same vibration conditions, yet they self-organize differently. The fcc structure has a width of six primitive cells, and the plane parallel to the page is the (100) plane. The higher compaction of the fcc structure is clearly observed if we compare the height of both phases in Fig. 2(c). Finally, if we add oil to the right vessel, two fcc structures are obtained [see Fig. 2(d)].

The above sequence clearly shows that the addition of oil triggers the transition from bct to fcc arrays. Three important aspects should be mentioned before we try to explain the origin of this transition. First, the oil added to the assemblies is uniformly distributed through all the beads by shaking the cell for a few minutes at a large Γ before the annealing is started. Second, while the exact amount of oil required to form the fcc cohesive structures is not crucial, if the system

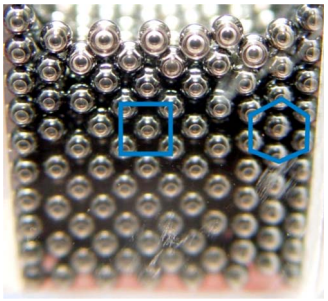

FIG. 3. (Color online) Cohesion is poor because the system is close to oil saturation. Therefore, bct and fcc phases coexist.

becomes saturated with too much, fcc structures are never formed. In Fig. 3 we show a structure, previous to saturation, where both bct and fcc phases coexist. Third, the polymorphism observed in the double container occurs thanks to the fortunate fact that the cross section of the vessels can be commensurate with both structures. This happens when $N_{\mathrm{bct}}\sqrt{3}\approx N_{\mathrm{fcc}}\sqrt{2}$, where N_x is the number of complete cells (bct or fcc). The reader can verify that this is satisfied for the following cases: $(N_{\mathrm{bct}},N_{\mathrm{fcc}})=(5,6),(9,11),(14,17),(18,22),(27,33),\ldots$.

IV. GRANULAR COHESION

It is well known that granulates change their mechanical properties when a small amount of liquid is added to them [20]. Liquid bridges between particles give place to capillary forces and, therefore, the granulates behave differently. Experience shows, for instance, that damp sand is better for making sandcastles than dry sand [21]. The packing of a powder is also affected by the addition of a liquid, especially in those cases where van der Waals forces are small [22]. The cohesive force between two particles consists of two parts: the surface tension σ acting at the wetting perimeter, and a term arising from the capillary pressure in the liquid [23,24]. The expression for this force is [25]:

$$F = \pi\sigma r_2(r_1 + r_2)/r_1), \tag{1}$$

where r_1 and r_2 are: $r[(1+h)\sec\beta-1]$ and $r[1+(1+h)\tan\beta-(1+h)\sec\beta]$, respectively, with $h=s/2r$, s the separation distance, r the radius of the spheres, and β the angle the meniscus makes with the surface of the bead (see inset in Fig. 4). In the literature on cohesive systems one normally finds plots of F vs β with s constant, or F vs s at constant β; the solid and dashed lines, respectively, in Fig. 4. But in practice, if we want to reproduce such plots in the laboratory with real data, we will need the continuous addition of the cohesive liquid. Indeed, if s varies, liquid has to be added in order to keep the meniscus with the same shape (constant β); if, instead, β varies, liquid has to be added in order to keep s constant. In our experiments, however, neither s nor β is constant, since liquid is not incorporated once the assemblies start the process of annealing.

We can evaluate the cohesive interaction in our assemblies by measuring the force between two isolated beads, as a function of s; see Fig. 5. This force is representative of the

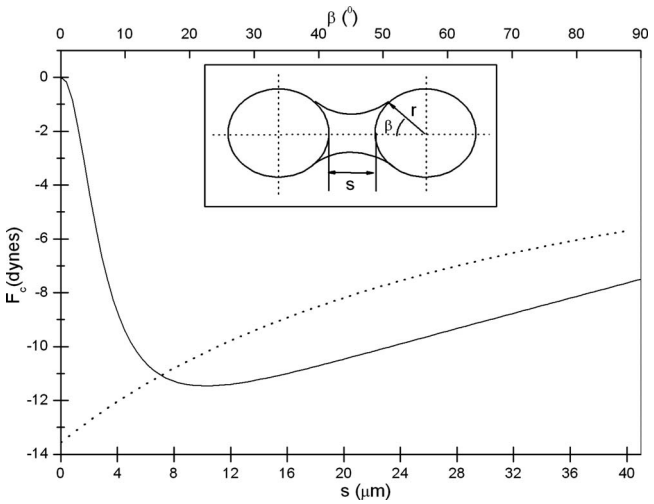

FIG. 4. Force between two cohesive spheres. The solid line is F vs β, keeping s constant. The dashed line is F vs s, keeping β constant. The cohesive bridge between the spheres is schematically depicted in the inset.

pairwise force acting on each particle during the annealing experiments. We observe that the force increases monotonically with s. In order to fit the data, we use the cohesive force given by Eq. (1), assuming a linear relationship between β and s (see the lower inset in Fig. 5). The value found for σ is in good agreement with the surface tension of the oil used in the experiments (28 dyn/cm). In Fig. 5 we also depict the hard-wall interaction between spheres when $s=0$.

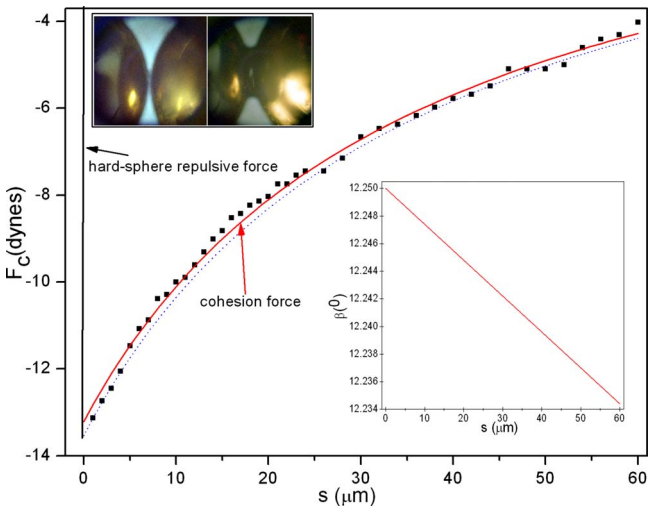

FIG. 5. (Color online) Experimental values for the cohesive force between two spheres (diameter 1.56 mm) as a function of s. The force was measured with an analytical balance and a micrometer. The continuous line is the best fit using the expression given by Eq. (1) (β is considered to change linearly with s, lower inset). The dashed line is the best fit using a constant value of β. The vertical line is the repulsive force during collisions. Two dry and cohesive touching spheres (upper inset), where the oil bridge is observed with a microscope. The thickness of the oil layer covering the cohesive spheres is around 10 μm. The surface tension is 28 dyn/cm.

V. FREE AND VIBRATIONAL ENERGIES

In general terms, the internal energy of a microscopic system is the sum of two contributions. The first contribution E_f accounts for the free energy of the system and is able to do work; the second, E_v, is associated with entropy and unable to do work. Due to the impossibility of reaching absolute zero temperature, a microscopic system will always have both energies. A granular system, however, is usually in "absolute" repose (at $\Gamma=0$), and its internal energy is equal to its free energy (gravitational, cohesive, or repulsive if the particles are charged). But if the system is vibrated, energy appears in the form of kinetic energy due to particle vibrations [26].

Building a theoretical framework to account for nonfree energies, relating these to entropy, and understanding the trade-off between free and nonfree energies in granular systems is beyond the aim of this paper. Nevertheless, the following experiments do support the idea that this mechanism exists, and here we aim to advance our understanding of this issue.

A. Dry assemblies

We vibrate two dry assemblies: rcp (before annealing) and bct (after annealing). These are vibrated at the same conditions, using a sinusoidal vertical vibration. The frequency and amplitude of the vibration are 100 Hz and 60 μm, respectively (corresponding to $\Gamma=2.4$). At these vibrating conditions, both structures are mechanically stable, meaning that no macroscopic bead rearrangements are observed. The only effect produced by the vibration is that the beads jiggle around their equilibrium positions, and this jiggling produces bead-bead and bead-wall collisions. The experiment consists simply in measuring, using an accelerometer (DeltaTron-BK, 1000 mV/g) attached to one of the walls of the container, the vibration produced by such collisions. If the vibrating material was a consolidated solid (for instance: the spheres of the assembly were glued together) the signal given by the accelerometer would be only the 100 Hz sinusoidal input vibration. A loose structure, however, will produce high-frequency noise superimposed on the sinusoidal signal. We find that a bct structure produces more jiggling than a rcp one (Fig. 6). The obvious conclusion is that the rcp structure is hindered with respect to the bct. This resembles the phenomenon occurring in hard-sphere suspensions, where due to geometrical arresting it is seen that a crystal has more vibrations than the glassy phase [16].

More experimental evidence is mounted in this direction: we filmed the vibrated structures with a high-speed charge-coupled device (CCD) camera (Photron DRS 512 $\times$512 pixels). Figure 7 depicts the x-y coordinates for two given spheres, one in the bct structure and the other in the rcp (see the insets), during 500 continuous frames taken at 1500 frames/s. Clearly, the wiggling areas are different. If we consider that a small wiggling area means vibrational arrest, it is clear that particles in the rcp structure are more arrested than particles in the bct crystal. Since the maximum vibration amplitude in this experiment is very small (60 μm), the phase separation observed in strongly vibrated granular systems (see Fig. 1 or Ref. [27]) is not observed here. Nevertheless, despite the homogeneity in the density of both structures, we take the precaution of following spheres located at the same height. In Fig. 8 we show the wiggling area during the same number of frames but this time averaged over 100 spheres. The results confirm the accelerometer measurements.

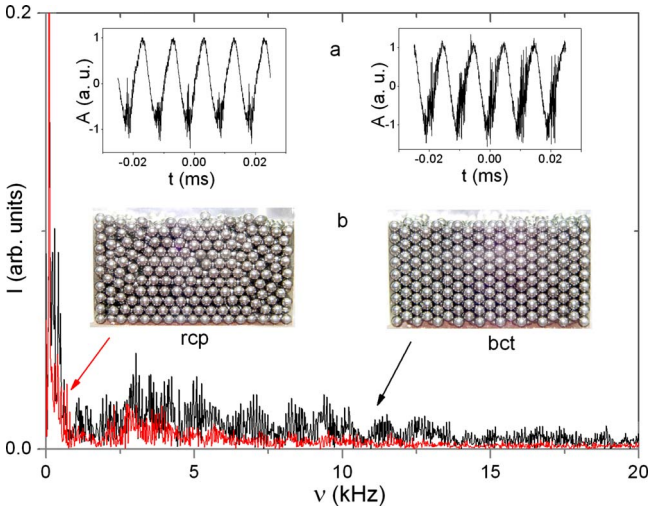

FIG. 6. (Color online) Fourier transforms of the vibration signal (inset a) produced by two different structures (inset b) when they are subjected to a sinusoidal vibration of 100 Hz and amplitude 60 μm. The red spectrum corresponds to the rcp and the black one to a bct phase. Due to jamming, the rcp structure produces less jiggling. The diameter of the spheres is 1.56 mm.

The internal energies of the vibrating rcp and bct structures are

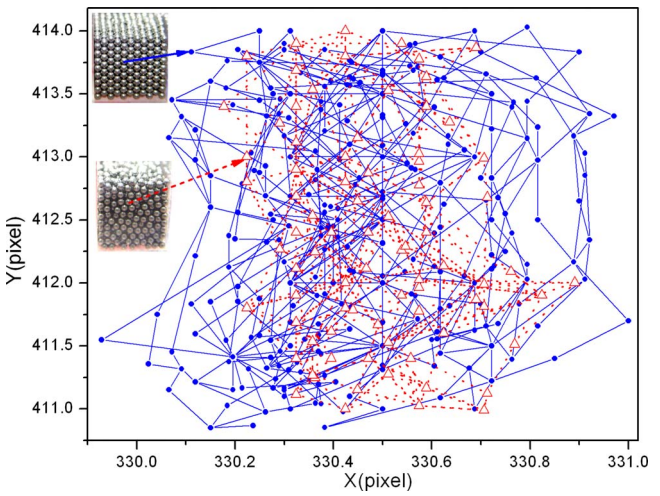

FIG. 7. (Color online) x-y coordinates of one sphere in the bct (dots) and rcp (triangles) structures, when they are subjected to vibration. The positions were taken using a fast camera at 1500 fps, but only 500 frames were used to obtain the coordinates. It is clear that the jiggling room for the rcp sphere is less than the one for the bct. The diameter of the spheres is 1.56 mm, equivalent to 29 pixels.

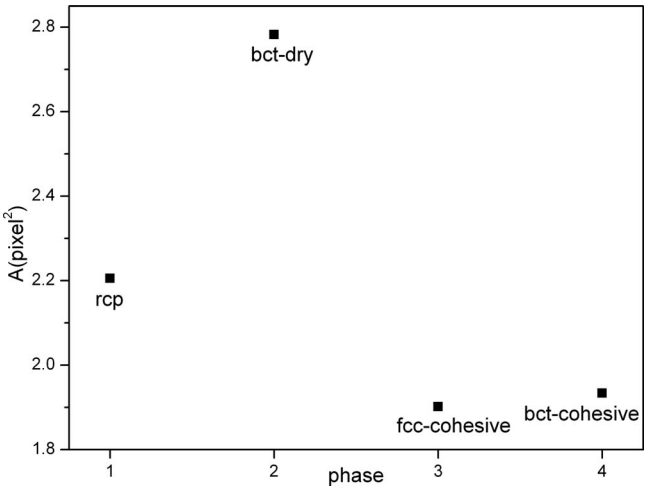

FIG. 8. Average jiggling area calculated for 100 spheres over 500 frames. The bct-dry structure gives the largest area and the fcc-cohesive structure the least. The size of the points indicates the error bars.

$$U_{\mathrm{rcp}} = \sum_i mgh_i^{\mathrm{rcp}} + E_v^{\mathrm{rcp}} \tag{2}$$

and

$$U_{\mathrm{bct}} = \sum_i mgh_i^{\mathrm{bct}} + E_v^{\mathrm{bct}}, \tag{3}$$

where the first and second terms in both equations are the gravitational and vibrational energies, respectively, h_i^{rcp} and h_i^{bct} the heights of the beads in the rcp and bct packings measured with respect to the bottom of the container, and m their mass. The difference in internal energies is

$$\Delta U^{\mathrm{bct\text{-}rcp}} = \sum_i mg(h_i^{\mathrm{bct}} - h_i^{\mathrm{rcp}}) + \Delta E_v^{\mathrm{bct\text{-}rcp}}. \tag{4}$$

B. Cohesive assemblies

Figure 9 shows the vibrational response of the bct (dry) and fcc (cohesive) structures. Clearly, the fcc structure vibrates almost like a consolidated solid (its response is quite sinusoidal), while the bct structure behaves like a loose material (its response is noisy).

The internal energy for the fcc cohesive vibrating packing is

$$U_{\mathrm{fcc}} = E_c^{\mathrm{fcc}} + \sum_i mgh_i^{\mathrm{fcc}} + E_v^{\mathrm{fcc}}, \tag{5}$$

where E_c^{fcc} is the cohesive energy of the structure, given by $\Sigma_j \int F_c ds$ (the sum is taken over all contacts), and E_v^{fcc} is the vibrational energy. The difference between bct and fcc internal energies is

$$\Delta U_{\mathrm{bct\text{-}fcc}} = \Delta E_c^{\mathrm{bct\text{-}fcc}} + \sum_i mg(h_i^{\mathrm{bct}} - h_i^{\mathrm{fcc}}) + \Delta E_v^{\mathrm{bct\text{-}fcc}}, \tag{6}$$

where E_c^{bct} is zero and E_c^{fcc} is a negative number.

Equation (6) can be written as $\Delta H = \Delta U - \Delta E_v$, where ΔH is the free energy difference. This equation is similar to the equation used in thermal systems, $\Delta H = \Delta U - T\Delta S$, where ΔH is the Helmholtz free energy difference and ΔS the change in entropy (at constant temperature).

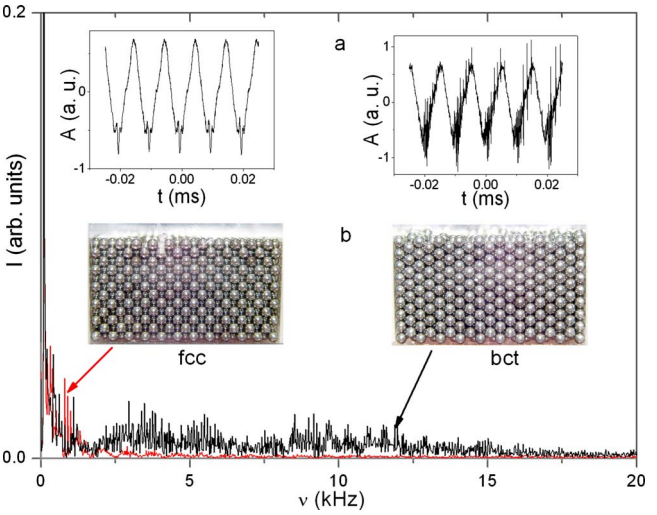

FIG. 9. (Color online) Fourier transforms of the vibration signal (inset a) produced by two different structures (inset b) when they are subjected to a sinusoidal vibration of 100 Hz and amplitude 60 μm. The red spectrum corresponds to the fcc cohesive and the black one to a bct structure. Due to the cohesive attractive force between the beads, the vibration signal for the fcc structure is lower. The diameter of the spheres is 1.56 mm.

Figure 10 summarizes what we have described above for dry and cohesive structures. From a dry bct to a cohesive fcc structure, the response of the accelerometer is shown when the structures are vibrated at 100 Hz and 60 μm of amplitude. The greater the high-frequency signal on top of the sinusoidal wave, the less consolidated is the assembly.

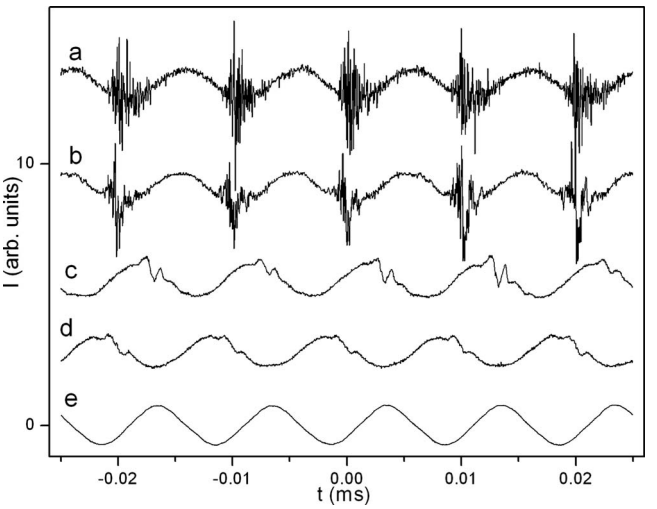

FIG. 10. Different structures: (a) bct-dry, (b) rcp-dry, (c) bct-cohesive, and (d) fcc-cohesive, vibrated at 100 Hz. An external accelerometer (mounted onto one of the walls of the container) captures the sum of the sinusoidal input signal of the vibration and the high-frequency contribution due to the jiggling of the beads. The larger this latter signal, the less consolidated is the assembly. Signal (e) is only for reference proposes; it corresponds to a fully consolidated structure.

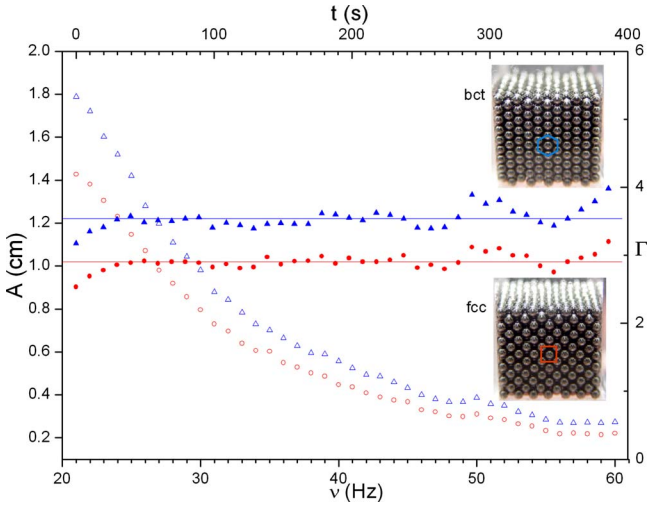

FIG. 11. (Color online) Two annealing processes at a different vibration strength Γ. The lower annealing (circles) was used to form the fcc crystal. If this is melted and recrystallized at a larger Γ (triangles), a different phase (bct) forms. The diameter of the spheres is 1.56 mm.

VI. PHASE TRANSITION

In the following final experiment we crystallize the fcc cohesive granular assembly shown at the bottom of Fig. 11. As shown in the figure, we do this by using the lower annealing curve (circles). Here, cohesion is needed to make the granular assembly organize into a fcc structure. However, if this structure is reannealed at a greater Γ (upper curve with triangles), the process renders a different phase: a bct crystal. It is remarkable that this phase transition occurs only by increasing the strength of the vibration. When there is no cohesion (the beads are dry), regardless of the value of Γ the annealing forms a bct crystal; but if cohesion is present, the system self-assembles into a fcc or a bct (for a greater Γ) structure. In other words, when the system is dry its energy landscape has only one global minimum (the bct phase), but it has two (bct and fcc) when there is cohesion. In order to go from one phase to the other there is a barrier to cross, and this is achieved by increasing the value of Γ.

This observation is crucial. The bct-fcc phase transition implies that the vibration energy, which is proportional to Γ, competes with the cohesive energy of the system. The result resembles what occurs in van der Waals systems, where temperature plays a thermodynamic role only because attractive energy is present. When the free energy is only gravitational (dry assemblies), the system is athermal, and Γ is only a control parameter.

As long as the particles are not too small [10], our results do not depend on the size and type of beads. It is important to remark as well that glass beads, which have a different restitution coefficient, render similar results to metallic beads. Furthermore, it might be argued that oil reduces the friction between beads and this could induce the self-assembling into fcc structures. However, graphite powder was used to reduce this friction and no fcc crystallization was observed [10]. Very recently we have also obtained fcc lattices if, instead of capillary cohesion, magnetic cohesion is used [28], confirming the fact that friction is not an important issue. Changes in the dissipation due to viscosity may play a role in the transition, but we believe that the underlying mechanism driving the transition is the change in free energy due to cohesion.

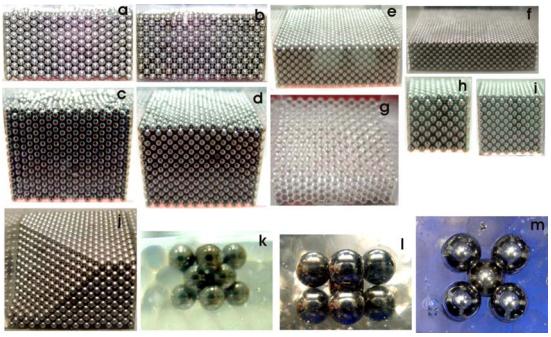

FIG. 12. (Color online) A collection of granular crystals of different sizes. (a) bct with 9 cells and (b) fcc with 11. Both have 2910 ball bearings of diameter 3.1 mm. (c) bct with 9 cells and (d) fcc with 11; both with 5026 ball bearings of diameter 1.56 mm. (e) fcc with 15 cells and 5291 ball bearings of diameter 1.56 mm. (f) fcc with 20 cells and 8405 ball bearings with diameter 1.56 mm. (g) fcc with 9 cells of 1243 glass spherical beads of diameter 4mm. (h) fcc with 5 cells with 666 ball bearings and (i) fcc with 7 cells and 1688 ball bearings, both having beads of the same diameter, 1.56 mm. (j) the (111) plane of the fcc crystal depicted in (d). (k) the unit cell of the fcc structure. This, made of ball bearings, is embedded in a fcc structure of glass beads. In order to observe it, glycerol is added to the container to match the refraction index of the glass beads. (l) Front view of the bct unit cell. (m) Top view of the bct unit cell.

In Fig. 12 we show a collection of different crystals. As long as an integer number of primitive cells fit commensurably inside a container, bct crystals of dry beads might be formed of any size. The same is valid for cohesive fcc crystals. The condition to grow bct and fcc crystals indiscriminately in the same container (as in Fig. 2) is satisfied only when these two integer numbers coincide within some tolerance (as discussed above). Figure 12(j) depicts a fcc crystal, where a cut has been done in order to show the (111) plane. This confirms that the crystals shown here are perfect arrays. Only one bead out of its position will make the structures clearly imperfect.

VII. CONCLUSIONS

We have studied the self-assembling of spherical beads by vibrational annealing and observed that dry beads form bct crystals. When oil (or water) is added to the system, the spheres subjected exactly to the same vibration protocol crystallize into fcc structures. We conclude that a trade-off between free (gravitational and cohesive) and nonfree (vibrational) energies takes place to reduce the free volume of the assemblies. Furthermore, when there is cohesion, the phase of the crystals can be selected by the strength of the annealing (Γ). In recent work, we observed that magnetic cohesion also induces self-organization into fcc structures, confirming our claim that cohesion is the true agent triggering fcc self-assembling [28].

Future work aims to simulate, by molecular dynamics, the self-assembling of the systems studied in this work. Evaluation of vibrational energies could help us to determine internal energies [Eqs. (2), (3), and (5)] and relate them to vibrational entropy changes. We hope that our results and conjectures may capture the interest of people working in statistical physics and granular materials.

ACKNOWLEDGMENTS

The paper was partly written during the sabbatical leave of one of us (J.C.R.S.) at the LMDH-PMMH (ESPCI), Paris, France. O.C. acknowledges financial support from CONACyT, Mexico. Fruitful discussions with A. Santos are acknowledged. This work has been supported by CONACyT, Mexico, under Grant No. 46709-F.

[1] E. Caglioti and V. Loreto, Phys. Rev. Lett. **83**, 4333 (1999).
[2] M. Nicodemi, A. Coniglio, and H. J. Herrmann, Phys. Rev. E **55**, 3962 (1997).
[3] E. Ben-Naim *et al.*, Physica D **123**, 380 (1998).
[4] G. D. Scott, Nature (London) **188**, 908 (1960).
[5] J. B. Knight, C. G. Fandrich, C. N. Lau, H. M. Jaeger, and S. R. Nagel, Phys. Rev. E **51**, 3957 (1995).
[6] S. F. Edwards and R. B. S. Oakeshott, Physica A **157**, 1080 (1989); M. Schröter, D. I. Goldman, and H. L. Swinney, Phys. Rev. E **71**, 030301(R) (2005).
[7] A. V. Anikeenko and N. N. Medvedev, Phys. Rev. Lett. **98**, 235504 (2007).
[8] O. Pouliquen, M. Nicolas, and P. D. Weidman, Phys. Rev. Lett. **79**, 3640 (1997).
[9] Y. Nahmad-Molinari and J. C. Ruiz-Suárez, Phys. Rev. Lett. **89**, 264302 (2002).
[10] O. Carvente and J. C. Ruiz-Suárez, Phys. Rev. Lett. **95**, 018001 (2005).
[11] J.-C. Tsai, G. A. Voth, and J. P. Gollub, Phys. Rev. Lett. **91**, 064301 (2003); A. B. Yu, X. Z. An, R. P. Zou, R. Y. Yang, and K. Kendall, *ibid.* **97**, 265501 (2006).
[12] C. P. Brock and J. D. Dunitz, Chem. Mater. **6**, 1118 (1994).
[13] R. E. Watson and M. Weinert, Phys. Rev. B **30**, 1641 (1984).
[14] E. Grunwald and C. Steel, J. Am. Chem. Soc. **117**, 5687 (1995).
[15] J. D. Dunitz, Chem. Biol. **2**, 709 (1995).
[16] D. Frenkel, Physica A **263**, 26 (1999).
[17] P. N. Pusey and W. van Megen, Nature (London) **320**, 340 (1986).
[18] E. R. Weeks *et al.*, Science **287**, 627 (2000).
[19] We used silicone oil with viscosity of 1 cP. Water also gives the same results, but in order to prevent oxidation of the beads, oil is preferred.
[20] T. G. Mason, A. J. Levine, D. Ertas, and T. C. Halsey, Phys. Rev. E **60**, R5044 (1999).
[21] A. J. Forsyth, S. R. Hutton, M. J. Rhodes, and C. F. Osborne, Phys. Rev. E **63**, 031302 (2001).
[22] C. L. Feng and A. B. Yu, Powder Technol. **99**, 22 (1998).
[23] R. Albert, I. Albert, D. Hornbaker, P. Schiffer, and A. L. Barabasi, Phys. Rev. E **56**, R6271 (1997).
[24] Strictly, the cohesive force also depends on the viscosity of the liquid. However, for the purpose of this study the viscous term is not considered.
[25] A. B. Yu, C. L. Feng, R. P. Zou, and R. Y. Yang, Powder Technol. **130**, 70 (2003).
[26] One could visualize this free energy by the following mental experiment: we suddenly remove the walls of the bed container to evaluate the work done by gravity in spreading the beads onto the vibrating table. The kinetic energy of the beads, due to vibration, will not change the results of the experiment. Thus, it will not contribute to the free energy.
[27] J. Bougie, S. J. Moon, J. B. Swift, and H. L. Swinney, Phys. Rev. E **66**, 051301 (2002).
[28] O. Carvente, J. M. Salazar, and J. C. Ruiz-Suarez (unpublished).